BJES Basrah Journal for Engineering Sciences

Basrah Journal for Engineering Sciences, Vol. 22, No. 2, (2022), 10-15

Original Article

Journal homepage: www.bjes.edu.iq
ISSN (Online): 23118385, ISSN (Print): 18146120

OPEN ACCESS

Thermal Analysis of a Perforated Vertical Wellbore

Haider Sami Mohammed [1,*], Hussein Sadiq Sultan [2], Emad Abdullah Khazal [3]

[1,2,3] *Department of Mechanical Engineering, College of Engineering, University of Basrah, Basrah, Iraq*

E-mail addresses: lec.haider.sami@uobasrah.edu.iq , hussein.sultan@uobasrah.edu.iq , emad.khazal@uobasrah.edu.iq

Received: 14 March 2022; Accepted: 10 April 2022; Published: 24 December 2022

Abstract

A numerical simulation of the effect evaluation of heat loss and temperature distribution along the wellbore is performed, for two models, the first is an open hole (without perforation) and the other is a perforated vertical wellbore. In this study, the Computational Fluid Dynamics (CFD) software code ANSYS FLUENT 15.0 has been used, for simulate a model of 3-D turbulent flow with stander k-ϵ model. The results of this show that, increasing the heat losses leads to an increase in the temperature gradient, while the temperature gradient decreases with increasing inlet main velocity. Also, the temperature of the produced crude oil decreases with increasing the length of the wellbore.

Keywords: Vertical wellbore, Perforation, Heat loss, CFD, Numerical.

https://doi.org/10.33971/bjes.22.2.2

1. Introduction

The fluid temperature enters into a variety of petroleum production operations calculations, including well drilling and completions, production facility design, controlling solid deposition, and analyzing pressure transient test data. Until the 1950, there were no substantial developments in this field except some unreliable laboratory-based correlations. In 1962, Ramey [1] presented the first transient heat transfer model of the vertical wellbore. He developed an approximate solution to the wellbore heat-transmission problem involved in injection of hot or cold fluids. The solution permits estimation of the temperature of fluids, tubing and casing as a function of depth and time. The result is expressed in simple algebraic form suitable for slide-rule calculation. The solution assumes that heat transfer in the wellbore is steady-state, while heat transfer to the earth will be unsteady radial conduction. The method used may be applied to derivation of other heat problems such as flow through multiple strings in a wellbore. Charles and Igbokoyi [2] developed the prediction model for flowing temperature distribution for a single-phase, two-phase, three-phase and identifying fluid type and properly analyzing its effect on temperature profile in the wellbore. The model can also be used to identify the parameters that affect the temperature profiles. The results showed that, there is a change in the temperature of the oil along the well, where the percentage of the decrease in the temperature from 152 °C to 138 °C, for a length of 4500 ft, and a flow rate of 4000 bbl/day. Xingkai et al. [3] studied the temperature distribution in the wellbore under different conditions using a designed horizontal well simulation experimental device. The experimental results were compared with the theoretical values. It was found that the error of the model was within 4%, which showed the reliability of predictions of the model. The experimental results showed that the Joule Thomson effect was significant in perforated wellbore. When the opening mode was the same, the larger the gas flow rate, the lower the temperature in the wellbore. Also, with the increase of liquid volume, the temperature drop effect decreased gradually. The more uniform the perforation distribution, the smaller the temperature change in the wellbore. With the increase of liquid volume, the influence of gas flow rate on temperature distribution decreased. The temperature gradient caused by Joule-Thomson effect decreased with the increase of wellbore holdup. Recently, Yang et al. [4] developed a transient heat transfer model for controlled gradient drilling. The model can be used to predict wellbore temperature distribution and to analyze the wellbore heat transfer efficiency for controlled gradient drilling. Tang et al. [5] developed three representative solutions for heat transfer in wellbore and formation: a fully numerical solution, a semi-numerical solution, and a fully analytical solution. These solutions play an important role in solving complex heat transfer models.

The aim of this research paper is to study the influence of heat loss and temperature distribution along the wellbore. Also, the effect of inflow velocity on the temperature distribution using the simulation program ANSYS FLUENT.

2. Numerical simulations

The rapid advancement of computer technologies and software enables the solution of theoretical simulations for complex applications. This paper investigates a thermal analysis of a single-phase flow through a vertical wellbore. The mathematical simulation with 3D model with turbulent flow in the vertical wellbore is performed. Using CFD ANSYS FLUENT. The vertical wellbore simulation is carried out using the conservation law (mass, momentum, and energy) in conjunction with the perturbation (k-ε) model [6].

The Finite Volume Method (FVM) solution of the continuity, momentum, energy, and turbulence model equations is used to explain the calculation process of the

control differential equation. The numerical analysis of the fluid flow field is solved using ANSYS FLUENT. The ANSYS FLUENT is used to solve the numerical analysis of the fluid flow field. The cell-vertex finite volume method is used by ANSYS FLUENT solvers. A fixed number of the control volumes are created from the fluid region.

3. Description of the models

In the current work, the numerical analysis is made with ANSYS FLUENT for two cases. The first was a numerical simulation of a vertical open hole is performed, to study the effect of heat loss and distribution of the crude oil temperature along the wellbore, for two models, the first is 0.1524 m diameter and 1 m length and the other with same diameter but 5 m length as shown in Fig. 1. The second case was the perforated vertical wellbore with 180° phase angle, for 20 spm. The vertical wellbore of (D = 0.1524 m) in diameter and of (L = 1 m) in length through axial centerline along the Y-axis, with perforations perpendicular on the vertical wellbore. The perforation diameter is 10 mm, length of perforation is 0.3 mm and the space vertical between each two successive perforations is (h) 0.1 m as shown in Fig. 2.

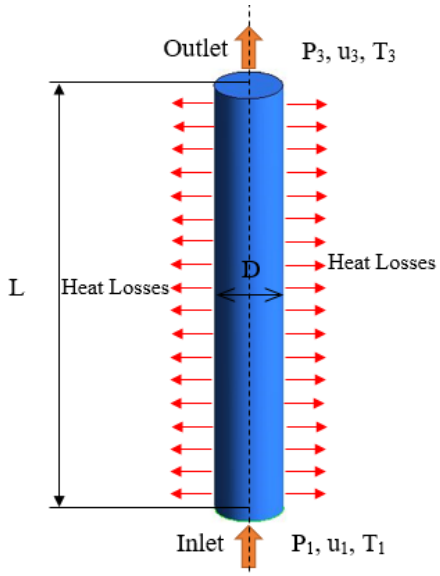

Fig. 1 geometry of open hole vertical wellbore with heat losses.

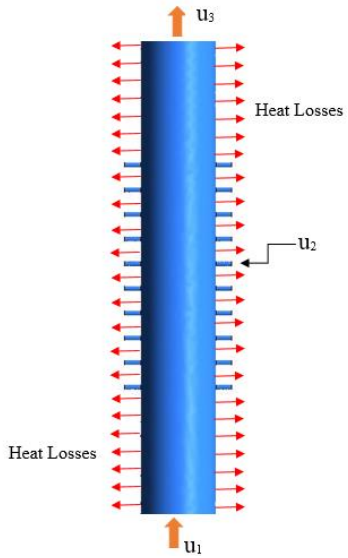

Fig. 2 geometry of a perforated vertical wellbore with heat losses.

4. Assumptions and simulation Parameters

The following assumptions are applied during the simulation. Three-dimensional steady flow for single-phase and Newtonian fluid flow. The gravity effect is neglected and the perforation is perpendicular to the direction of the wellbore fluid flow. The working fluid is crude oil, the crude oil properties and production casing are given in Table 1.

Table 1. the crude oil properties and production casing.

Properties	Crude Oil	Production casing
Density (kg/m^3)	842	8030
Viscosity (kg/m.s)	0.006	-
Specific Heat (J/kg.K)	2182	502.48
Conductivity (W/m.K)	0.145	16.27
Temperature inlet (K)	338	-

5. Boundary conditions

The governing equations system in CFD can be solved only if there are boundary conditions to fulfill a solution. Therefore, we need to provide boundary conditions to a CFD solver. There are various forms of boundary inputs that convert a real situation to its CFD model counterpart.

ANSYS FLUENT allows several methods for the definition of a fluid boundary. In this study, use the boundary conditions given below:

1. The inlet velocity of the wellbore (u_1) is 1.5 m/s.
2. The outlet pressure (P_3) of the wellbore is equal to zero.
3. The roughness of casing wall is 0.02 mm, and different heat losses.
4. Constant heat flux.
5. No slip velocity at walls.

6. Governing equations

Fluid flow in a perforated vertical wellbore undergoes a significant physical change which including pressure change due to friction losses in vertical wellbore and perforations, acceleration, and mixing. Also, temperature and enthalpy change due to heat exchange between the wellbore and its surrounding formation. To properly describe these physical changes, the three governing equations of this fluid's flow are (mass, momentum, and energy equations) [7, 8 and 9].

- **Conservation of Mass:** The mass conservation equation describes the fluid inflow velocity and density change along the wellbore. It is expressed by the equation below:

$$\rho \frac{\partial}{\partial x_i}(u_i) = 0 \tag{1}$$

- **Conservation of Momentum:** The momentum conservation equations in the Cartesian coordinate are given below:

$$\frac{\partial}{\partial t}(\rho u_i) + u_j \frac{\partial(\rho u_i)}{\partial x_j} = -\frac{\partial P}{\partial x_i} + \frac{\partial}{\partial x_j}(\tau_{ji}) + F_i \tag{2}$$

- **Conservation of Energy:** The equation for conservation of energy is described as follows:

$$\frac{\partial}{\partial x_i}(\rho u_i T) = \frac{\partial}{\partial x_i}\left(\Gamma \frac{\partial T}{\partial x_i}\right) + S_T \quad (3)$$

- **Turbulence Models (Standard *k-ϵ* model):** The standard *k-ϵ* model belongs to the general class of two-equation models, which deal with two distinct transport equations and are most commonly used in industrial applications due to their economy, robustness, and reasonable accuracy. The model's first is major assumption is that the turbulent viscosity μ_t isotropic. The second major assumption is that dissipation and production terms given in the k equation are approximately equal locally [10].

The standard *k-ϵ* model uses the following transport questions for *k*:

$$\rho u_j \frac{\partial k}{\partial x_j} = \frac{\partial k}{\partial x_j}\left(\left(\mu + \frac{\mu_t}{\sigma_k}\right)\frac{\partial k}{\partial x_j}\right) + 2\,\mu_t S_{ij}.S_{ij} - \rho\epsilon \quad (4)$$

and ϵ;

$$\rho u_j \frac{\partial \epsilon}{\partial x_j} = \frac{\partial \epsilon}{\partial x_j}\left(\left(\mu + \frac{\mu_t}{\sigma_\epsilon}\right)\frac{\partial \epsilon}{\partial x_j}\right) + C_{1\epsilon}\frac{\epsilon}{k}\mu_t S_{ij}.S_{ij} - C_{2\epsilon}\rho\frac{\epsilon^2}{k} \quad (5)$$

The tensor of the strain rate can be expressed in terms of velocity.

$$S_{ji} = \frac{1}{2}\left(\frac{\partial u_j}{\partial x_i} + \frac{\partial u_i}{\partial x_j}\right) \quad (6)$$

The equations (4), and (5) include five constants [11]. The amounts of these constants are:
$\sigma_k = 1.00$, $\sigma_\epsilon = 1.30$, $C_\mu = 0.09$, $C_{1\epsilon} = 1.44$ and $C_{2\epsilon} = 1.92$

7. Grid independence test

To ensure the results of the numerical solution using ANSYS FLUENT 15.0 software. The second step of numerical simulation is to identify the maximum mesh size. In this study, ICEM CFD is used to generate the mesh with different maximum mesh size. The varying the maximum size of the mesh is applied to illustrate the best mesh properties which can be used to simulation for all cases in this work.

The geometry of fluid flow is a vertical pipe of 1 m length and 0.1524 m diameter, with 2 perforations at center vertical distance and 180º perforations phase angle. The perforation diameter is 0.01 m and length is 0.032 m from the pipe surface. The boundary condition for this case, the inlet velocity from main pipe is 1.5 m/s, inlet velocity from each of perforation is 2 m/s, and the outlet pressure is equal to zero.

The grid independency of all the mesh size is based on the average static pressure at two locations, the first location at the inlet of the pipe and the second location at a point in the middle of line as shown in Fig. 3. Table 2 in appendix 1 explained the information of the grid independence test.

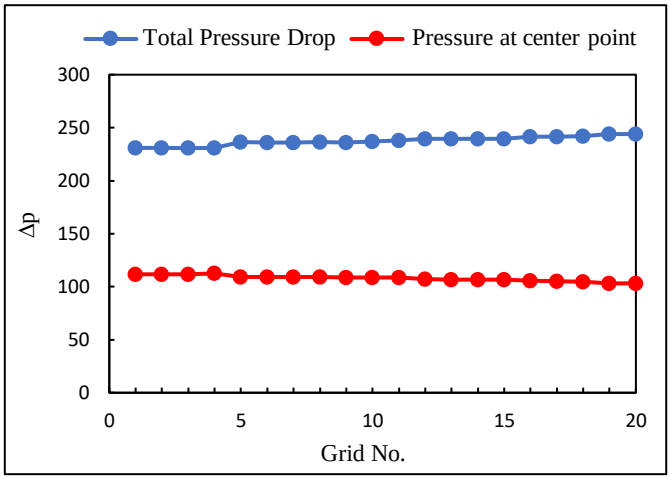

Fig. 3 comparison of static pressure for varying mesh sizes.

Twenty values for the maximum mesh size were tested. The grid independency error of the predicted average static pressure lies between the previous and the next of the maximum mesh size at 0.00575 (Grid 13) with 199945 nodes and 308020 elements. The percentage error between grid 13 and grid 14 for the two locations are 0.01 % for the inlet of pipe and 0.08 % for the point in the middle of the line. The maximum mesh size of 0.006 is used in the simulation in order to obtained good accuracy results. For checking quality, the determinant of element obtained equal to 0.775 at least, while the value acceptable in ICEM CFD must be greater than 0.1, then the mesh quality is good acceptable.

8. Model validation

In order to verify the accuracy of the CFD model. A comparison with the results of Salim et al. [12] is performed. The flow geometry is a 3D vertical pipe with two perforations at middle and the diameter of the perforations are 0.012 m; length is 0.15 m and 180º the perforations phase angle. The diameter of the pipe is 0.2 m and the length is 1 m. The boundary conditions of this validation are as follow; inlet mean velocity (u_1 = 2.5 m/s), inlet velocity from perforations (u_2 =1 m/s), while the static pressure at the outlet equal to zero. Fig. 4 shown the results of this validation for the static pressure drop along the centerline of the pipe, the results show a good agreement with the work of Salim et al., and the percentage error between Salim et al. and present work is less than 1.6 %.

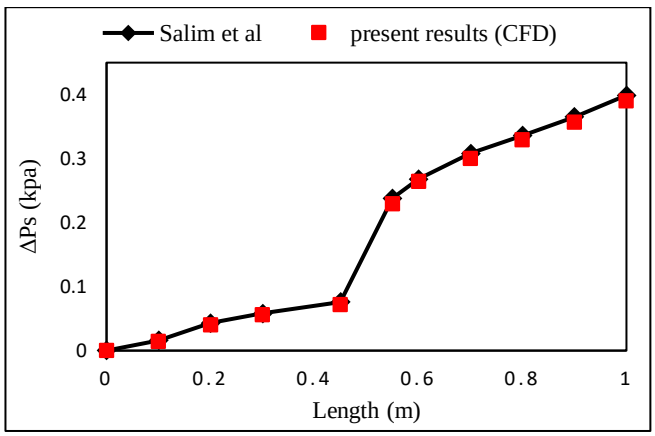

Fig. 4 Comparison between the present work and the data of Salim et al.

9. Results and discussion

9.1. Open hole vertical wellbore

Fig. 5 shows the variation of the temperature gradient of the crude oil with the heat losses. For two inlet velocities of 1 and 1.2 m/s and the outlet pressure is equal to zero. It is noticed that, the temperature gradient increases with increasing heat losses. Also, an increase of inlet velocity leads to a decrease in temperature gradient, due to an increased inflow rate.

Fig. 6 represents the temperature contour along the wellbore with a velocity of 1 m/s and the outlet pressure is equal to zero. It is shown that, the heat transfers in the radial direction and the greatest temperature in the center of the wellbore.

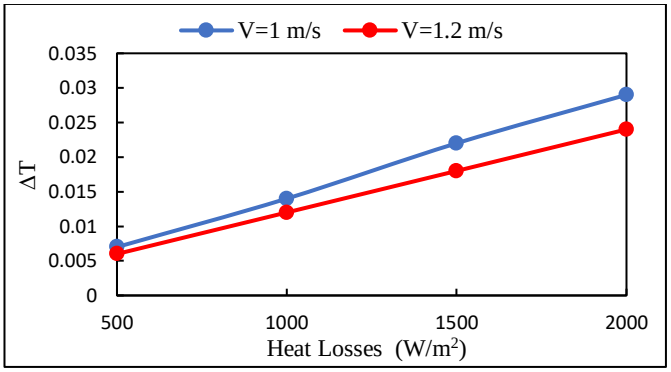

Fig. 5 the variation of the temperature gradient with the heat losses.

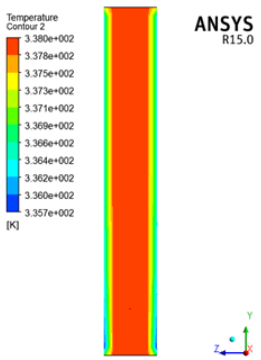

Fig. 6 temperature contour of crude oil through the vertical open hole.

Fig. 7 illustrates the temperatures distribution at the centerline along open hole vertical wellbore with a length of 10 m. It is clear that, the temperature decreases with increasing the length of the well, due to the increase of the surface area of the wellbore casing, this causes an increase in heat losses. Also, increasing inlet velocity leads to decreased temperature, due to increasing the mass flow rate with constant heat loss.

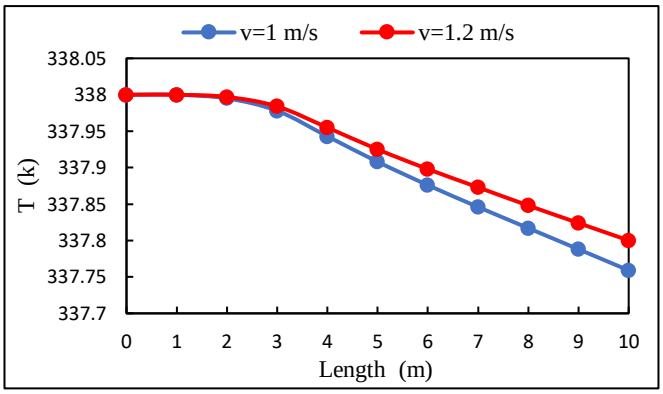

Fig. 7 the temperature distribution with the length of open hole vertical wellbore.

9.2 The perforated vertical wellbore

In this part, the effect of heat losses of a perforated vertical wellbore with 20 spm and 180° perforations phase angle is studied. Fig. 8 shows the variation total temperature drop with heat losses. The total temperature drop increases with increasing heat losses, due to increase of heat losses with constant a flow rate.

Fig. 9 illustrates contour of temperature distribution along 1 m vertical wellbore with 20 spm. It is shown that, the heat transfers in the radial direction and the greater temperature in the center of the wellbore.

Fig. 10 shows temperature distribution contour along 1 m vertical wellbore with 20 spm and heat losses at wall is equal to 5 kW. The temperature at inlet and outlet of the wellbore is 338 K, while the inlet temperature of perforation is 350 K. It is clear that the temperature of the crude oil entering from the perforations into the wellbore decreases, due to the difference between the temperature of the crude oil in the wellbore with the temperature of the crude oil the entering from the perforations.

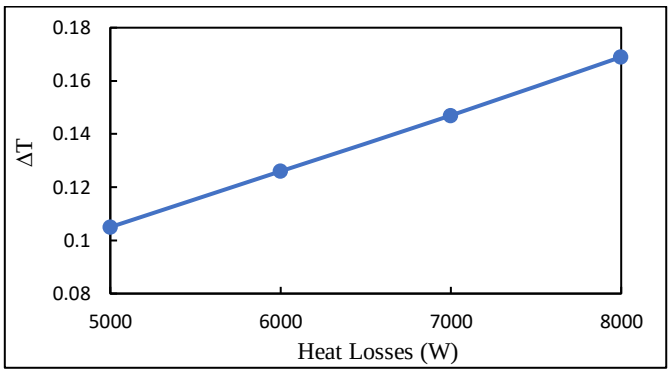

Fig. 8 the variation of the total temperature drop with heat losses.

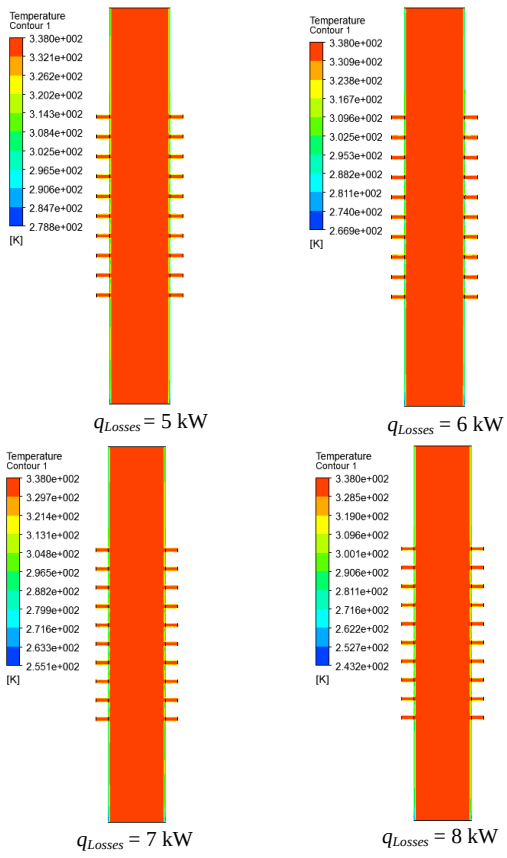

Fig. 9 temperature contour with different heat losses and 20 spm.

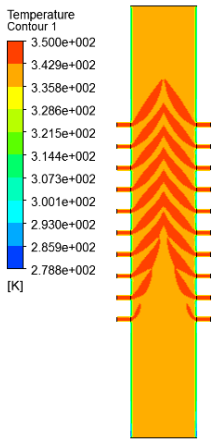

Fig. 10 temperature contour with q_{Losses} = 5 w and T_p = 350 K.

10. Conclusions

In this study, the numerical simulation of the open hole and a perforated vertical wellbore with thermal load are performed using ANSYS FLUENT program. From the results of this study, the following conclusions are obtained:

1. The temperature gradient increases with increasing heat losses.
2. The temperature gradient decreases with increasing inlet main velocity.
3. The temperature of the produced crude oil decreases with increasing the length of the wellbore.
4. Increasing the temperature of the perforations leads to a decrease in the temperature gradient.

Nomenclature		
Symbol	**Description**	**Unit**
A	Area	m^2
D	Wellbore Diameter	m
d	Perforation Diameter	m
g	Gravitational Acceleration	m/s^2
L	Wellbore Length	m
l_p	Perforation Length	m
n	Number of Perforation	1/m
Y	Dimensional Coordinates	m
Greek Symbols		
Symbol	**Description**	**Unit**
ΔP	Pressure Drop	Pa
θ	Perforation Phase Angle	deg.
μ	Fluid Viscosity	kg/m.s
ρ	Density	kg/m^3
Subscripts		
Symbol	**Description**	
1	Inlet	
2	Perforation	
3	Outlet	
i, j, k	Vector	
p	Perforated	
w	Wall	
T	Total	
Abbreviations		
Symbol	**Description**	
CFD	Computational Fluid Dynamic	
FVM	Finite Volume Method	
spm	Shot Per Meter	
spf	Shot Per Foot	
C.V	Control Volume	

References

[1] H. J. JR. Ramey, "Wellbore Heat Transmission", Journal of Petroleum Technology, Vol. 14, No. 4, pp. 427-435, April 1962. https://doi.org/10.2118/96-PA

[2] Y. O. Charles, and A. O. Igbokoyi, "Temperature Prediction Model for Flowing Distribution of Wellbores and pipelines", Nigeria Annual International Conference and Exhibition, Lagos, Nigeria, August 6-8, 2012. https://doi.org/10.2118/163038-MS

[3] X. Zhang, Z. Jiang, R. Liao, B. Shi, L. WU, K. Liu, and Y. Zhang, "Study on Temperature Distribution of Perforated Horizontal Wellbore", Journal of Thermal Science, Vol. 29, pp. 194-205, 2019. https://doi.org/10.1007/s11630-019-1247-9

[4] H. Yang, J. Li, and G. Liu, "Development of transient heat transfer model for controlled gradient drilling", Applied Thermal Engineering, Vol. 148, pp. 331-339, 2019. https://doi.org/10.1016/j.applthermaleng.2018.11.064

[5] H. Tang, B. Xu, and A. Rashid Hasan, "Modeling wellbore heat exchangers fully numerical to fully analytical solutions", Renewable Energy, Vol. 133, pp. 1124-1135, 2019. https://doi.org/10.1016/j.renene.2018.10.094

[6] FLUENT Inc., FLUENT 6.3 User's Guide, 2006.

[7] M. A. Abdulwahid, S. F. Dakhil, and I. N. Niranjan Kumar, "Numerical Simulation of Flow through Wellbore for Horizontal Wells", WIT Transactions on Modelling and Simulation, Vol. 55, pp. 127-138, 2013. https://doi.org/10.2495/CMEM130111

[8] M. A. Abdulwahid, S. F. Dakhil, and I. N. Niranjan Kumar, "Numerical analysis of fluid flow properties in a partially perforated horizontal wellbore", American Journal of Energy Engineering, Vol. 2, Issue 6, pp. 133-140, 2014. https://doi.org/10.11648/j.ajee.20140206.12

[9] T. Vyzikas, "Application of numerical models and codes", MERiFIC, Marine Energy in Far Peripheral and Island Communities, February 2014. https://archimer.ifremer.fr/doc/00324/43550/43111.pdf

[10] H. K. Versteeg, and W. Malalasekera, An Introduction to Computational Fluid Dynamics, Second Edition, Pearson Education Limited, Prentice Hall, 2007. ISBN: 978-0-13-127498-3

[11] S. E. Haaland, "Simple and Explicit Formulas for the Friction Factor in Turbulent Pipe Flow", Journal of Fluids Engineering, Vol. 105, Issue 1, pp. 89-90, 1983. https://doi.org/10.1115/1.3240948

[12] Mohammed K. Salim, "Numerical Simulation of Perforated Vertical Wellbore", M. Sc. thesis, Mechanical Engineering Department, University of Basrah, April 2017.

Appendix 1

Fig. 11 and Fig. 12 shows the ICEM CFD interface and mesh distribution for some models with different phase angle.

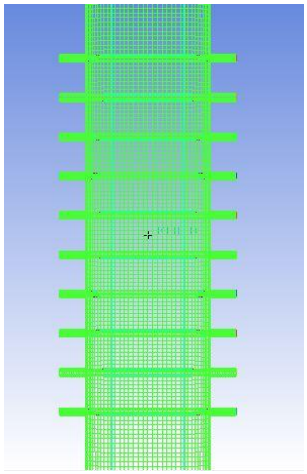

Fig. 11 ICEM CFD interface in ANSYS FLUENT with 3D model for two perforations with 180° phase angle. The type of meshing is the Hexahedral.

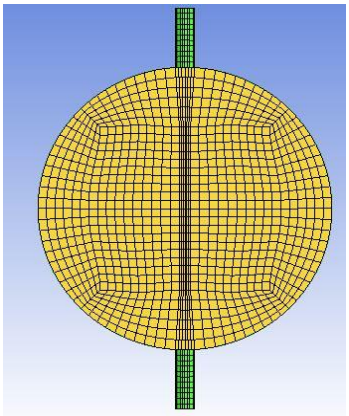

Fig. 12 The ICEM mesh for 180° phase angle.

Table 2. the information of the grid independence test.

Grid No.	Max size	Nodes	P drop (Pa)	P center (Pa)
1	0.009	75251	230.901	111.512
2	0.00875	77599	230.962	111.601
3	0.0085	82494	230.722	111.637
4	0.00825	91150	231.025	112.545
5	0.008	102688	236.537	109.012
6	0.00775	111409	235.781	109.291
7	0.0075	114493	235.825	109.239
8	0.00725	122458	236.302	109.252
9	0.007	141119	236.054	108.874
10	0.00675	144699	237.011	108.812
11	0.0065	155800	238.116	108.671
12	0.00625	182209	239.374	106.951
13	0.006	199945	239.339	106.856
14	0.00575	216052	239.327	106.792
15	0.0055	246013	239.251	106.783
16	0.00525	284608	241.581	105.681
17	0.005	323851	241.638	105.336
18	0.00475	358883	241.829	104.608
19	0.0045	435186	243.884	103.394
20	0.00425	481412	243.934	103.153